ACS Catalysis

Research Article

pubs.acs.org/acscatalysis

Active Sites of Pd-Doped Flat and Stepped Cu(111) Surfaces for H_2 Dissociation in Heterogeneous Catalytic Hydrogenation

Qiang Fu[†,‡] and Yi Luo*[,†,‡]

[†]Hefei National Laboratory for Physical Sciences at the Microscale, University of Science and Technology of China, Hefei 230026, Anhui, P. R. China

[‡]Department of Theoretical Chemistry and Biology, School of Biotechnology, Royal Institute of Technology, S-106 91 Stockholm, Sweden

Supporting Information

ABSTRACT: It has been shown in recent experiments that the Cu(111) surface doped by a small amount of Pd atoms can exhibit excellent catalytic performance toward the dissociation of H_2 molecules. Here we performed systematic first-principles calculations to investigate the corresponding mechanism. Our results clearly demonstrate that a very small number of Pd atoms in the subsurface layer can effectively reduce the energy barrier of H_2 dissociation, making the ensembles composed of the surface and contiguous subsurface Pd atoms as the active sites. The catalytic activity can be further improved if the Pd atoms are doped in the stepped Cu surfaces. The impact of the subsurface Pd atoms comes from an enhanced surface−adsorbate interaction caused by adjusting the electronic structure of the substrate. The important role played by the subsurface atoms offers an efficient approach to finely tune the surface activity by a very limited number of atoms. Our findings should be very useful for understanding and improving the catalytic properties of alloy systems for the industrially important hydrogenation reactions.

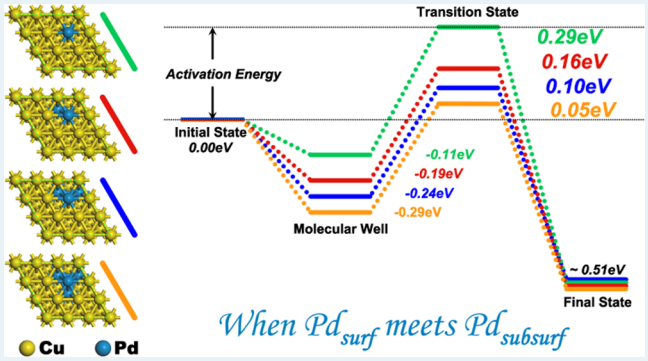

KEYWORDS: *hydrogenation, active site, density functional theory, subsurface atom, bimetallic alloy*

1. INTRODUCTION

In heterogeneous catalysis, the ensemble of a small number of atoms often acts as the active site and usually plays an essential role in catalytic reactions.[1−3] The determination of the structure and the composition of such active sites is crucial for understanding and improving the properties of the catalysts.[4,5] In recent decades tremendous progress has been made in experiments to elucidate the active sites and the reaction mechanisms,[6−14] thanks to the great advent of the atomically resolved *in situ* spectroscopies and the various surface science techniques.[15−17] However, it is still difficult, if not impossible, to reveal all the mechanistic details from the experiments alone.[18] Fortunately, theoretical calculations provide a complement and usually indispensable way to investigate the catalytic phenomena. With this approach the nature of the active site can be probed, and even be designed to achieve superior catalytic performance benefited from the revealed reaction mechanisms.[19−24] Thus, through the combination of experimental and theoretical efforts, one would expect to achieve significantly improved performance of the catalysts for a number of industrially important chemical reactions.

Catalytic hydrogenations have huge applications in food, petrochemical, and pharmaceutical industries. In these processes the dissociation of hydrogen molecule is often known to be a vital step, for which much effort has been devoted to developing novel catalysts with superior properties.[25−27] One effective strategy is to dope a small amount of precious metal into the common elements.[27−34] A recent breakthrough has shown experimentally that the doped Pd atoms can effectively promote H_2 dissociation and spillover on the Cu(111) surface.[34] Not only does the very small quantity of the precious palladium element allow a more cost-effective catalyst, but more remarkably, it makes the hydrogenation reaction very selective, which offers a more nature friendly way in the practical applications with much reduced byproduct waste.[34] The outstanding catalytic performance of the Pd-doped Cu(111) surface has been firmly verified in the experiments.[31,34] However, the actual structure of the active site to catalyze H_2 dissociation still remains unknown. The individual isolated Pd atom in the topmost layer was initially proposed as the active site with the corresponding barrier as low as 0.02 eV,[31] but later calculations showed that at this site the activation energy, that is, the energy difference between the transition state and the initial state with molecule far away from the surface,[35] is in fact up to 0.25 eV.[36] The theoretically estimated catalytic activity is thus much lower than that

Received: April 9, 2013
Published: April 26, 2013

   dx.doi.org/10.1021/cs400267x | ACS Catal. 2013, 3, 1245−1252

revealed from the experiments.[31,36] This strongly implies that the isolated surface Pd atom might not be the true active site as has been expected.[31,34,36]

To resolve this contradiction, we performed systematic first-principles calculations to investigate the H_2 dissociation on the Pd-doped Cu(111) surfaces. Our results clearly demonstrate that only the ensembles composed of surface and contiguous subsurface Pd atoms can act as the active sites. It is found that a very small number of Pd atoms in the subsurface layer can effectively reduce the energy barrier of H_2 dissociation, contributing to the production of H atoms, the vital step in the heterogeneous hydrogenation. Such effect comes from the enhancement of the interaction between the adsorbate and the substrate, indicating that surface reactivity can be finely tuned by very limited subsurface atoms.

2. COMPUTATIONAL METHODS

Our calculations are performed using the Vienna ab initio simulation package (VASP),[37,38] within the framework of density functional theory (DFT). The effects of spin polarization have been taken into account but are found to be negligible. The projector augmented wave (PAW) pseudopotentials are employed to represent the interaction between the core ions and the valence electrons.[39] The exchange correlation effects are mainly described by the functional GGA-PW91,[40] while GGA-PBE[41] has also been used in some configurations to compare the activation energies from difference functionals. The equilibrium lattice constant of Cu is calculated to be 3.636 Å, in good consistency with previous calculations.[42,43] Dipole corrections for the electric potential and total energy have been applied to eliminate the spurious dipole−dipole interactions along the vertical direction between image supercells.

To model the flat (111) terrace, we use a supercell containing four atomic layers of a (3 × 3) unit cell and a 14 Å-thick vacuum region. For the description of the (211) surface, that is, the one modeling the step edge formed by two (111) terraces, 12 atomic layers of a (3 × 1) unit cell plus a 13 Å-thick vacuum region are employed. The energy cutoff for the plane-wave basis sets is set to be 400 eV, and the Brillouin zone sampling is carried out using the (6 × 6 × 1) Monkhorst−Pack grids. During the optimizations, the uppermost two/six layers of (111)/(211) surface as well as the adsorbate are allowed to move until the maximum value of the force is below 0.02 eV/Å. The transition states of H_2 dissociation are located by the climbing-image nudged elastic band method[44] and are further verified by the Dimer method.[45]

The scanning tunneling microscopy (STM) image is simulated using the Tersoff−Hamann theory, through the integration of the spatially resolved density of state (DOS) within the energy range from a bias potential to the Fermi level.[46] The simulations of X-ray photoelectron spectroscopy (XPS) are carried out with Kresse's approach.[47,48] In this method, the XPS peaks are calculated by comparing the core-level bonding energy (E_{CL}) of the element under different environments.[47] The value of the E_{CL} is determined by the energy difference between two states.[47] The first one is the electronic ground state, while the second corresponds to the state in which one electron is removed from the core of the atom and added to the valence or conduction band.[47] Since only the relative shifts of the E_{CL} are relevant in VASP calculations,[48] the $3d_{5/2}$ XPS peaks of Pd are obtained by comparing their own values with the one of the Pd(111) surface, calibrated by the experimental value of 334.88 eV.[49]

In the ab initio molecular dynamics (AIMD) simulations, the flat (111) terrace is modeled by four atomic layers of a large (6 × 6) unit cell, separated by a 14 Å-thick vacuum region, with the top two layers free to move. The energy cutoff for the plane-wave basis sets is set to be 300 eV, and the Brillouin zone sampling is carried out using the (2 × 2 × 1) Monkhorst−Pack grids. The MD simulations are performed within the micro-canonical ensemble using a time step of 1 fs. These are constant energy molecular dynamics simulations, in which the calculated Hellmann−Feynman forces are used to control the motion of the atoms. The H_2 molecule is initially placed in a horizontal orientation and 4 Å above the surface (see Supporting Information, Figure S1), moving toward the topmost Pd atoms along the surface normal. The kinetic energy of the H_2 molecule is changed from 0.1 to 0.3 eV, without vibrational or rotational excitations. The zero-point motion of H_2 is also not considered, which in fact leads to a better agreement with the quantum dynamical simulations.[50,51] The MD simulation ends when the H_2 molecule returns to the initial distance of 4 Å from the surface or the two H atoms have been diffusing for a sufficient long time after dissociation. No recombination of the two hydrogen atoms has been observed during the diffusion. It should be noted that since the purpose of our AIMD simulations is not for the calculation of the H_2 dissociation probability, whose experimental value has not been measured yet, but for the demonstration of the effectiveness of Pd ensembles toward H_2 dissociation, other initial orientations of H_2 molecule are not taken into account.

3. RESULTS AND DISCUSSION

3.1. Structure of the Active Sites. The Cu(111) surface is relatively inert for the dissociation of the H_2 molecule, for which an activation energy up to 0.46 eV is obtained from our calculations (Figure 1a). When an individual Pd atom is doped

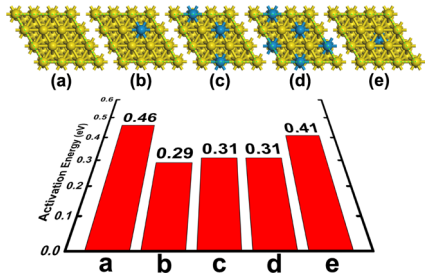

Figure 1. Structures of the clean (a) and the Pd-doped Cu(111) surfaces with different doping patterns (b−e). The activation energies of H_2 dissociation for the five configurations are shown at the bottom. The yellow and blue spheres represent the Cu and the Pd atoms. The green dotted line labels the unit cell in the calculations.

in the topmost layer of Cu(111), the value of the energy barrier decreases to 0.29 eV (Figure 1b). These calculated activation energies agree very well with previous calculations.[36] The reduction of the energy barrier means that a single doped isolated Pd atom can effectively increase the activity of the inert Cu surface, but not to the level revealed by the experiments.[31,34] In other words, the isolated single surface Pd atom is not the key active site in the H_2 dissociation. We have then gradually increased the concentration of the surface Pd atoms in our calculations, as schematically shown in Figure 1c and Figure 1d. It should be noted that the nearest-neighbor arrangement is not taken into account since such a pattern has

dx.doi.org/10.1021/cs400267x | ACS Catal. 2013, 3, 1245−1252

been firmly excluded by the experiments.[29,31,34,52] We find that the energy barrier of H_2 dissociation cannot be reduced with the increase of the surface Pd concentration. Moreover, a single Pd atom doped in the sublayer of Cu(111) is also considered in the model of Figure 1e. It can be seen that such a configuration is much less reactive than the surface doped by a topmost Pd (Figure 1b). One can thus conclude that the isolated Pd atoms in Cu(111) are not responsible for the superior catalytic activity revealed experimentally for the dissociation of the H_2 molecule.[31,34]

In experiments it has been observed that during the deposition process a part of the Pd atoms goes into the sublayers of Cu(111),[31,34,52] and as a result, the surface and subsurface Pd atoms are both present in the alloy systems. The catalytic activity of individual Pd atoms in the topmost layer has aroused a great deal of attention;[29,31,34] however, until now the possible effect of the sublayer Pd atoms on the catalytic H_2 dissociation has been ignored. We now turn our attention to the structures that consist of Pd atoms at both the surface and the subsurface layers (see Figure 2). The results from the

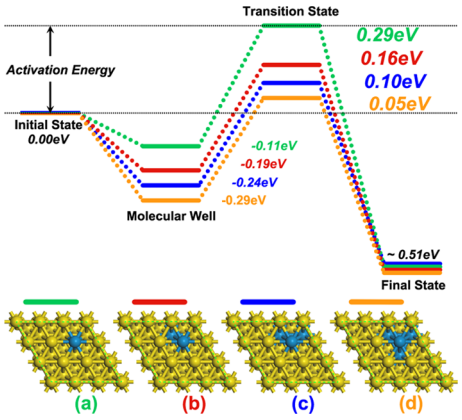

Figure 2. Energy profiles of H_2 dissociation on a series of Pd-doped Cu(111) surfaces: (a) only one surface Pd atom (green); (b) one surface plus one subsurface Pd atoms (red); (c) one surface plus two subsurface Pd atoms (blue); and (d) one surface plus three subsurface Pd atoms (orange). The activation energy and the energy of the molecular well in H_2 dissociation are also shown in the profiles. In the configurations (b), (c), and (d), the surface and the subsurface Pd atoms are connected to each other.

individual doped topmost Pd (Figure 1b) are also shown in Figure 2a for comparison. We first tried a two-atom ensemble including one surface and one subsurface Pd atoms connected with each other as shown in Figure 2b. It is quite interesting to observe that in this case the activation energy of H_2 dissociation can decrease to 0.16 eV. When a third Pd, connecting with both the two existing Pd atoms, is introduced into the sublayer (Figure 2c), the activation energy further reduces to 0.10 eV. This seems to suggest that the energy barrier decreases with the increment of the subsurface Pd atoms that are directly bonded with the surface Pd. To verify it, we introduced the fourth Pd atom in the sublayer as shown in Figure 2d. Indeed, the activation energy now becomes as low as only 0.05 eV. It should be mentioned that such a value of the energy barrier agrees very well with the one from the experiments.[31,34] We have also used the other functional, GGA-PBE,[41] to calculate the activation energy. The same values of energy barrier are obtained. It strongly indicates that an ensemble involving both the surface and the nearby subsurface Pd atoms could be responsible for the high catalytic activity of the Pd-doped Cu surface toward H_2 dissociation.

In fact, the ensemble of the doped Pd atoms, which exists in both the toplayer and the sublayer of the Cu(111) surface, can adopt a variety of configurations, not limited to the three cases shown in Figure 2 b–d. In particular, the surface and the subsurface Pd atoms may be either joined together or unconnected to each other. Therefore a series of structures that involve both the surface and the subsurface Pd atoms should be taken into account, as shown in Figure 3. These

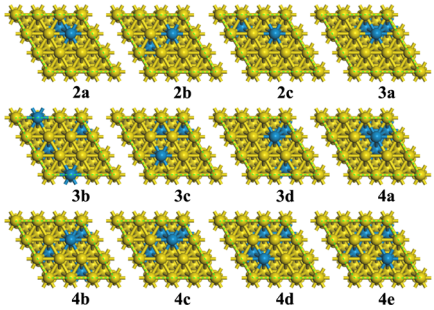

Figure 3. Series of Pd-doped Cu(111) alloys with different doping patterns combining both the surface and the subsurface Pd atoms. In the label of the different configurations, the Arabic numeral ***n*** represents the number of the doped Pd atoms, with ***1*** surface and ***n-1*** subsurface Pd atoms. The English alphabet refers to the different configurations with the same number of doped Pd atoms.

configurations not only include the three ones in Figure 2 b–d (labeled as 2a, 3a, and 4a) but also consist of several new geometries, in which not all of the Pd atoms are connected with each other. The energy profiles of H_2 dissociation on these configurations are explored, and the key values, that is, the H_2 adsorption energy (the opposite value of the molecular well energy) and the activation energy, are listed in Table 1. An

Table 1. Adsorption Energies of H_2 Molecule ($E_{ad}(H_2)$) and the Activation Energy of H_2 Dissociation (E_b(disso)) for the Configurations As Shown in Figure 3

	$E_{ad}(H_2)$ (eV)	E_b(disso) (eV)
2a	0.19	0.16
2b	0.11	0.29
2c	0.09	0.30
3a	0.24	0.10
3b	0.10	0.20
3c	0.10	0.20
3d	0.17	0.14
4a	0.29	0.05
4b	0.21	0.06
4c	0.27	0.03
4d	0.20	0.08
4e	0.10	0.16

important finding is that only the configuration, in which the surface Pd connects with at least one subsurface Pd atom, has a low activation energy value. The results clearly demonstrate that these joint surface-subsurface Pd ensembles can all play a role as the active site in the dissociation of H_2 molecule.

dx.doi.org/10.1021/cs400267x | ACS Catal. 2013, 3, 1245–1252

3.2. STM and XPS Simulations. The facileness of H_2 dissociation on the Pd-doped Cu surface was first revealed by STM.[31,34] We have simulated STM images for various configurations, displayed in Figure 4, to compare with the

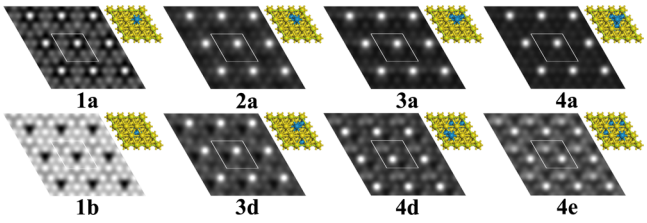

Figure 4. Simulated STM images (bias: −0.20 eV) for the Pd-doped Cu(111) surface of different doping patterns. Labels of these configurations are the same as the ones in Figure 3. 1a (1b) represents the structure with only one Pd atom doped in the top (second) layer of the Cu(111) surface.

experiments.[31,34] One can see that an individual Pd atom appears as a protrusion in the topmost layer (1a in Figure 4), and as a depression at the subsurface (1b in Figure 4). The simulated results agree very well with the measurements.[31] It is worth noting that in experiments these features were used to distinguish between topmost Pd and Pd atom in the second layer.[31] However, when the Pd atoms from both surface and subsurface layers are simultaneously involved in the configurations, the situation becomes complicated, and no simple one-to-one mapping exists between the structure and the STM image. For example, when a different number of subsurface Pd atoms connect with the topmost Pd, as shown in 2a, 3a, and 4a of Figure 4, the configurations have very similar STM image. The topmost Pd atom again shows a protrusion, the same as the isolated Pd (1a), but there is no distinct feature to identify the subsurface Pd atoms. As a result, it is not easy to determine how many Pd atoms are located in the second layer and how they connect with the surface Pd, although the brightness of the protrusion could increase to a certain extent with the increment of the subsurface Pd atoms. The STM image becomes even more complicated when the surface and subsurface Pd atoms are separated in the structures. For instance, for the configurations 3d and 4d in Figure 4, each one has a depression in the theoretical STM image, which is very similar to the one for the isolated subsurface Pd (1b). However, there is no Pd atom in the area with these two dark points, showing that the depression in the STM image does not necessarily correspond to the Pd atom in the subsurface layer. In addition, the area with no topmost Pd can also appear as a protrusion, as shown in the simulated image of 4e in Figure 4. The complexity of the above results indicates that the STM image alone can not provide a comprehensive picture on the detailed structures of the Pd-doped Cu(111) surface.

X-ray photoelectron spectroscopy (XPS), a quantitative method to analyze the elemental composition as well as its chemical and electronic state, is a commonly used technique for the investigation of surface structure. Since XPS characteristics of the atom are usually related to the environment that it locates, different structures of the surface can thus be distinguished by XPS experiments. For this purpose, we have simulated the XPS of the topmost Pd atom in various configurations, and listed the position of the Pd $3d_{5/2}$ peak in Table 2. It is interesting to find that the Pd $3d_{5/2}$ peaks are sensitive to the configurations, and can be classified into four

Table 2. Simulated $3d_{5/2}$ XPS Peaks of the Topmost Pd Atom for the Different Configurations of the Pd-Doped Cu(111) Surface[a]

group	configuration	Pd $3d_{5/2}$ XPS (eV)
group 1	1a	335.79
	2b	335.80
	2c	335.80
	3b	335.76
	3c	335.75
	4e	335.70
group2	2a	335.66
	3d	335.65
	4b	335.60
	4d	335.58
group3	3a	335.55
	4c	335.50
group4	4a	335.46

[a]The results are classified into four groups according to the similarity of the geometries. Labels of these configurations are the same as the ones in Figures 3 and 4.

groups accordingly. From Table 2 one can see that the topmost Pd atom with no subsurface Pd connecting below has the largest core-level bonding energy, locating in the range from 335.70 to 335.80 eV (Group 1). When the topmost Pd bonds with one subsurface Pd atom, its $3d_{5/2}$ peak has a red shift of 0.1 eV, and then locates between 335.58 to 335.66 eV (Group 2). The $3d_{5/2}$ peak continues to move toward the lower energy range with the increment of the subsurface Pd atoms, and finally locates at 335.46 eV when the three subsurface atoms right below are all replaced by Pd (Group 4). Overall, the $3d_{5/2}$ XPS peak of the topmost Pd atom is sensitive to the configurations; however, since the largest binding energy shift is only 0.3 eV, it is still not easy to distinguish the various configurations in the experiments.

3.3. Mechanism for the Improvement of the Catalytic Activity. From Figure 2 one can see that with the increment of the Pd atoms at the subsurface layer, the energies of the molecular well and the transition state decrease accordingly. The stabilization of the transition state results in the reduction of the activation energy and therefore a facile H_2 dissociation. Such stabilization comes from the enhancement of the interaction between the surface and the adsorbate, which can then be well described by the value of the H_2 adsorption energy. According to the *d* band model of chemisorption, the interaction strength between the transition metal surface and the adsorbate can be determined by the electronic structure of the surface itself, that is, the position of the d band relative to the Fermi level.[53,54] The upshift of the d state usually corresponds to the increase of the surface−adsorbate interaction.[53,54] From the correlation relation in Figure 5a for all of the considered Pd doped Cu(111) surfaces, one can clearly see that the adsorption energy of the H_2 molecule, the symbol of the interaction strength, increases with the moving up of the d band center. More remarkably, the data points in Figure 5a can be divided into three groups: the region I, II, and III. In region I, the three points have the highest d band center and therefore the largest adsorption energy. These three points come from the configurations 3a, 4a, and 4c, respectively, in Figure 3, in which more than two subsurface Pd atoms connect with the topmost Pd. In region II, the four points have the intermediate d band center and the adsorption energy,

dx.doi.org/10.1021/cs400267x | ACS Catal. 2013, 3, 1245−1252

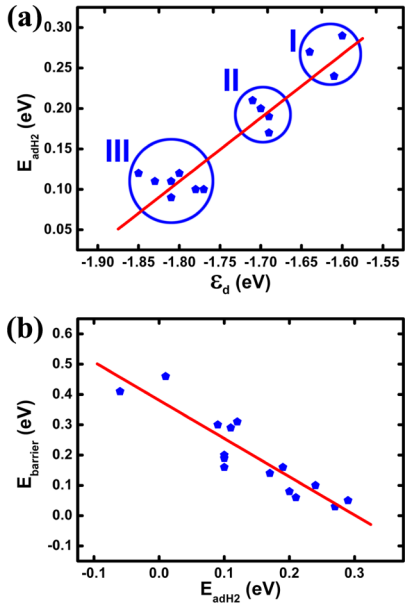

Figure 5. (a) Correlation relation between the d band center of the doped top Pd atom and the adsorption energy of H_2 molecule (the opposite value of the molecular well energy). (b) The correlation between the energy barrier of H_2 dissociation (activation energy) and the H_2 adsorption energy on a series of Pd-doped Cu(111) surface.

corresponding to the geometries 2a, 3d, 4b, and 4d, respectively, in Figure 3, in which only one subsurface Pd atom bonds with the topmost Pd. In region III, the seven points have the lowest d band center and the adsorption energy. In these structures, the surface and subsurface Pd atoms do not connect with each other. From the above analysis, we can draw the conclusion that with the increment of the subsurface Pd atoms bonded directly to the topmost Pd, the d band center of the top Pd atom moves up, resulting in the enhancement of the surface−adsorbate interaction and the reduction of the activation energy.

In Figure 5b we plot the activation energy of H_2 dissociation against the H_2 adsorption energy. Between these two sets of data a linear correlation is found, in which higher adsorption energy corresponds to lower activation energy. This relation makes the H_2 adsorption energy a good "descriptor" to describe the catalytic activity of the Pd-doped Cu(111) surfaces toward the dissociation of H_2 molecule. Since it is much easier and more computational efficient to calculate the adsorption energy than the activation energy, such relation will be very helpful for the fast screening of active component in Pd or other precious metal doped Cu surfaces.

3.4. Molecular Dynamics Simulations. To verify the catalytic activity of different configurations furthermore, we have carried out AIMD simulations to study H_2 dissociation on four representative structures given in Figure 2, which contain one surface and a different number of subsurface Pd atoms underneath. To be consistent with the labels in Figure 3, the structures are also denoted as 1a, 2a, 3a, and 4a for zero, one, two, and three subsurface Pd atoms, respectively. The initial kinetic energy of the H_2 molecule is varied between 0.10 and 0.30 eV, while the evolution of the two hydrogen atoms is shown in Figure 6. One can see that the H_2 molecule can dissociate on all of the four surfaces when its initial kinetic energy reaches 0.30 eV, a value larger than all four activation energies (Figure 6a). When the initial kinetic energy is reduced

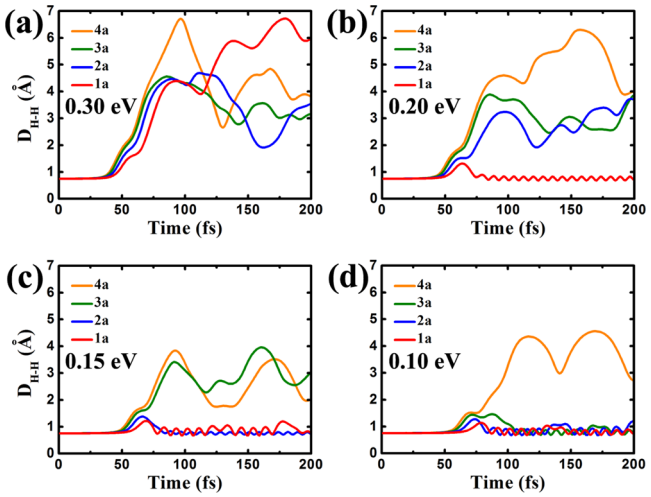

Figure 6. Evolution of the distance between the two hydrogen atoms during the AIMD simulations on the four representative surfaces. Only the first 200 fs is shown here. Labels of the configurations are the same as the ones in Figure 4, corresponding to the four structures in Figure 2. Different initial kinetic energies of (a) 0.30 eV, (b) 0.20 eV, (c) 0.15 eV, and (d) 0.10 eV are used in the simulations.

to 0.20 eV, the structure 1a, having one topmost Pd only, cannot make H_2 dissociate (Figure 6b). On this configuration the approaching molecule elongates its H−H bond up to 1.31 Å, and then bounces back from the surface with part of its translational energy transferring to the vibrational degrees of freedom. When the initial kinetic energy is reduced to 0.15 eV, the reflection of the H_2 molecule also occurs on the structure 2a (one surface Pd plus one subsurface Pd below), with the H−H bond elongated to 1.38 Å as H_2 approaches the surface (Figure 6c). On the configuration 1a, the dissociation of H_2 cannot take place either; but in contrast to 2a, the H_2 molecule is first trapped by the surface Pd atom for 183 fs, with its vibrational degree of freedom excited, before it scatters back from the surface. Then we further reduce the initial kinetic energy of H_2 to 0.10 eV. On the structures 2a and 1a, the H_2 molecule eventually bounces back from the surface after being trapped by the topmost Pd for 639 and 420 fs, respectively. On the configuration 3a, the situation is a bit complicated. It is found that the H_2 molecule can elongate its H−H bond to 1.46 Å, a value very close to the one of the transition state, and then is trapped by the topmost Pd for a long time, exciting the stretching vibration of the H_2 molecule. We have not observed the H_2 dissociation or reflection up to 3200 fs. In this case the quantum tunneling effect is expected to play a major role in the breaking of the H−H bond. It is striking to see that with this initial kinetic energy the H_2 molecule can still dissociate easily on the structure 4a that is composed of one surface Pd and three underlying subsurface Pd atoms (Figure 6d). It is worth noting that according to the Boltzmann distribution, the number of the H_2 molecule decays exponentially with the increment of its kinetic energy. Thus in reality most of the H_2 molecules are expected to dissociate on the ensembles with much lower activation energy, for example, the ones composed of surface and contiguous subsurface Pd atoms. These configurations would play a much more important role than the isolated topmost Pd atom on the catalytic dissociations of H_2 molecule.

3.5. Catalytic Activity of the Stepped Cu(111) Surface. In experiments it was revealed that the step edge of Cu(111) is

dx.doi.org/10.1021/cs400267x | ACS Catal. 2013, 3, 1245−1252

the place where Pd atoms get into the host Cu surface.[31,34] The evaporated Pd atom, randomly walking on the terrace, can be trapped at the neatest ascending step edge, and exchange with the Cu atoms.[34] This Pd-doped Cu structure at the step edge may also have remarkable catalytic performance toward H_2 dissociation, and should not be overlooked.

We employed the (211) surface to describe the step edge, formed by two (111) terraces separated by a monatomic step. The corresponding energy profiles of H_2 dissociation are shown in Figure 7. On the clean Cu(211) surface, even the step edge is

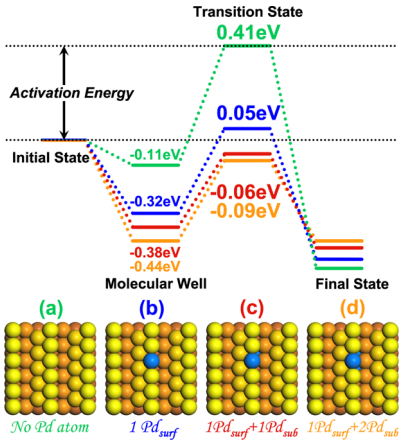

Figure 7. Energy profiles of H_2 dissociation on a series of stepped (211) alloy surfaces: (a) no Pd atom (green); (b) only one surface Pd atom (blue); (c) one surface and one subsurface Pd atom below (red); (d) one surface and two subsurface Pd atoms below (orange). The activation energy and the energy of the molecular well in H_2 dissociation are also shown in the profiles. The yellow (blue) spheres represent the Cu (Pd) atoms. The deepening of the yellow color represents the reduction of the height.

involved in H_2 dissociation (Figure 7a), the activation energy is still relatively high, being 0.41 eV compared with the value of 0.46 eV on the flat Cu(111). Doping an isolated Pd atom into the ridge of the step edge changes the situation significantly (Figure 7b). In this case the activation energy decreases to only 0.05 eV, much lower than the value of 0.29 eV on the flat one. When another Cu atom, located below and connecting with the topmost Pd, is also substituted (Figure 7c), the energy barrier of H_2 dissociation becomes as low as −0.06 eV. It should be noted that now the transition state has already had a lower energy than the initial state, that is, the one when H_2 is far away from the substrate. Such result means that to overcome the energy barrier, in principle no extra energy needs to be provided. In other words, on such kind of surface the H_2 molecule can dissociate spontaneously. When the third Cu, connecting with both the two Pd atoms, is also replaced by Pd (Figure 7d), the energy barrier further reduces to −0.09 eV. Thus, by comparing the activation energy between the stepped and the flat surface, one can clearly see that doping the Pd atoms in the step edge is a more effective way to catalyze H_2 dissociation. It means that in practical applications the Cu nanoparticles, doped by a small amount of Pd, may exhibit more excellent activity than the extended surfaces, on which remarkable catalytic performance have already been experimentally demonstrated. Our results provide a feasible approach to further improve the catalytic properties of the Cu−Pd alloy systems.

To investigate the structural feature of the active site on the stepped (211) surface, a range of different configurations has been taken into account, as shown in Figure 8. The key values

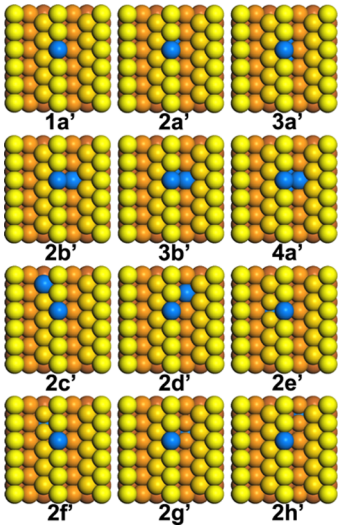

Figure 8. Series of stepped alloy surfaces with different doping patterns combining both the surface and the subsurface Pd atoms. The naming rule is the same as the ones in Figure 3, that is, the Arabic numeral ***n*** represents the number of the doped Pd atoms, with ***1*** surface and ***n-1*** subsurface Pd atoms. The English alphabet refers to the different configurations with the same number of doped Pd atoms.

of the energy profile, that is, the H_2 adsorption energy and the activation energy, are listed in Table 3. We first consider one

Table 3. Adsorption Energies of H_2 Molecule ($E_{ad}(H_2)$) and the Activation Energy of H_2 Dissociation (E_b(disso)) for the Stepped Surfaces As Shown in Figure 8

	$E_{ad}(H_2)$ (eV)	E_b(disso) (eV)
1a′	0.32	0.05
2b′	0.30	0.07
2a′	0.38	−0.06
3b′	0.37	−0.06
3a′	0.44	−0.09
4a′	0.42	−0.08
1a′	0.32	0.05
2c′	0.32	0.06
2d′	0.30	0.06
2e′	0.32	0.05
2f′	0.30	0.10
2g′	0.30	0.06
2h′	0.31	0.07

type of subsurface Pd atom, which connects with but does not locate below the topmost Pd, as shown in the structures of 2b′, 3b′, and 4a′, to compare with the ones of 1a′, 2a′, and 3a′, respectively. It can be seen that the adsorption energy and the dissociation barrier are almost the same between the two sets of structures, which indicates that the participation of such kind of subsurface Pd does not affect the H_2 dissociation. Then we examine another type of subsurface Pd atoms, which do not connect with the topmost Pd, as shown in the structures of

dx.doi.org/10.1021/cs400267x | ACS Catal. 2013, 3, 1245−1252

2c′−2h′. By comparing the energy values with the one of 1a′, one can see that the existence of these subsurface Pd atoms cannot reduce the activation energy either. From these results, we reach the conclusion that on stepped Cu(211), the ensembles composed of surface Pd and subsurface Pd atoms right underneath play the role of active sites in the dissociation of H_2 molecule.

In Figure 9a, we plot the correlation between the H_2 adsorption energy and the d band center of the topmost Pd atom. The results from the stepped (211) surface and the flat (111) terrace are shown together for comparison. One can see that the two sets of data points follow the same linear relation. In the case of the stepped surface, the d band center also moves up with the increment of the subsurface Pd atoms, which locate right below the topmost Pd, resulting in the enhancement of the interaction between the H_2 molecule and the substrate. This implies that the mechanism to improve the catalytic properties by the doping Pd atoms in the subsurface layer is the same as the one that we have discussed for the flat (111) terrace. It is striking to see that by doping a very small number of Pd atoms in the subsurface layer of Cu surfaces, one can systematically increase the H_2 adsorption energy from 0.09 eV to 0.44 eV, and correspondingly decrease the activation energy of H_2 dissociation from 0.29 eV to −0.09 eV through the modification of the surface electronic structures. In Figure 9b, we show the correlation between the dissociation barrier and the adsorption energy, for both the stepped (211) and the flat (111) surface. Because the local structure of the transition state is different from each other, the two sets of data points are placed on two straight lines, showing a weak geometric effect in the correlation relations.[22] For each structure, the adsorption energy of the H_2 molecule is still a good "descriptor" to describe the catalytic activity of the alloy surfaces, quite useful for the fast screening of the active components to design better catalysts.

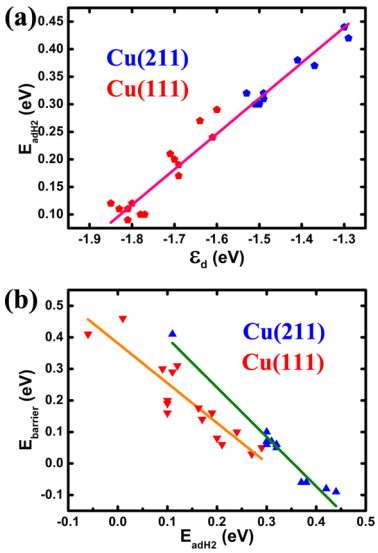

Figure 9. Correlation relation for the stepped (211) surfaces (blue points). The results from the flat (111) terraces (red points) are also shown for comparison. (a) the relation between the d band center of the topmost Pd and the H_2 adsorption energy; (b) the relation between the activation energy of H_2 dissociation and the H_2 adsorption energy.

4. CONCLUSIONS

In summary, we have identified the true active site of the Pd-doped Cu(111) surfaces for H_2 dissociation. Our calculations have revealed the decisive role of the subsurface Pd atoms in improving the catalytic performance, in particular for the stepped Cu surface. The high catalytic activity of such ensembles composed of the surface and contiguous subsurface Pd atoms comes from the enhanced surface−adsorbate interaction, owing to the upshift of the d band state through the substitution of Pd atoms. Our results clearly show that the surface activity of the Pd-doped Cu surfaces can be well modified by a very limited number of subsurface Pd atoms, implying that the subsurface-atom doping can be used as an efficient approach to finely tune the surface activity of alloy systems. This work would be crucial in rational design of novel catalysts with superior performance for the industrially important hydrogenation reactions.

■ ASSOCIATED CONTENT

Supporting Information

A figure of the initial orientation of the H_2 molecule in the AIMD simulations. This material is available free of charge via the Internet at http://pubs.acs.org.

■ AUTHOR INFORMATION

Corresponding Author

*E-mail: luo@kth.se.

Notes

The authors declare no competing financial interest.

■ ACKNOWLEDGMENTS

This work is supported by the Major State Basic Research Development Programs (2010CB923300), the National Natural Science Foundation of China (20925311), Göran Gustafsson Foundation for Research in Natural Sciences and Medicine, and the Swedish Research Council (VR). The Swedish National Infrastructure for Computing (SNIC) is acknowledged for the supercomputer resources.

■ REFERENCES

(1) Taylor, H. S. *Proc. R. Soc. Lond. A.* **1925**, *108*, 105−111.
(2) Boudart, M. *Adv. Catal.* **1969**, *20*, 153−166.
(3) Boudart, M., Djéga-Mariadassou, G., Eds.; *Kinetics of Heterogeneous Catalytic Reactions*; Princeton University Press: Princeton, NJ, 1984.
(4) Somorjai, G. A. *Introduction to Surface Chemistry and Catalysis*, 1st ed.; Wiley: New York, 1994.
(5) Santen, R. A.; Neurock, M. *Molecular Heterogeneous Catalysis: A Conceptual and Computational Approach*, 1st ed.; Wiley-VCH: Weinheim, Germany, 2006.
(6) Zambelli, T.; Wintterlin, J.; Trost, J.; Ertl, G. *Science* **1996**, *273*, 1688−1690.
(7) Hansen, P. L.; Wagner, J. B.; Helveg, S.; Rostrup-Nielsen, J. R.; Clausen, B. S.; Topsøe, H. *Science* **2002**, *295*, 2053−2055.
(8) Mitsui, T.; Rose, M. K.; Fomin, E.; Ogletree, D. F.; Salmeron, M. *Nature* **2003**, *422*, 705.
(9) Ackermann, M. D.; Pedersen, T. M.; Hendriksen, B. L. M.; Robach, O.; Bobaru, S. C.; Popa, I.; Quiros, C.; Kim, H.; Hammer, B.; Ferrer, S.; Frenken, J. W. M. *Phys. Rev. Lett.* **2005**, *95*, 255505.
(10) Matthiesen, J.; Wendt, S.; Hansen, J. Ø.; Madsen, G. K. H.; Lira, E.; Galliker, P.; Vestergaard, E. K.; Schaub, R.; Laegsgaard, E.; Hammer, B.; Besenbacher, F. *ACS Nano* **2009**, *3*, 517−526.

(11) Fu, Q.; Li, W. X.; Yao, Y. X.; Liu, H. Y.; Su, H. Y.; Ma, D.; Gu, X. K.; Chen, L. M.; Wang, Z.; Zhang, H.; Wang, B.; Bao, X. H. *Science* **2010**, *328*, 1141−1144.
(12) Zhai, Y. P.; Pierre, D.; Si, R.; Deng, W. L.; Ferrin, P.; Nilekar, A. U.; Peng, G. W.; Herron, J. A.; Bell, D. C.; Saltsburg, H.; Mavrikakis, M.; Flytzani-Stephanopoulos, M. *Science* **2010**, *329*, 1633−1636.
(13) Green, I. X.; Tang, W. J.; Neurock, M.; Yates, J. T. *Science* **2011**, *333*, 736−739.
(14) Behrens, M.; Studt, F.; Kasatkin, I.; Kühl, S.; Hävecker, M.; Abild-Pedersen, F.; Zander, S.; Girgsdies, F.; Kurr, P.; Kniep, B. L.; Tovar, M.; Fischer, R. W.; Nørskov, J. K.; Schlögl, R. *Science* **2012**, *336*, 893−897.
(15) Somorjai, G. A.; Park, J. Y. *Phys. Today* **2007**, *60*, 48−53.
(16) Tao, F.; Salmeron, M. *Science* **2011**, *331*, 171−174.
(17) Grunwaldt, J.; Wagner, J. B.; Dunin-Borkowski, R. E. *ChemCatChem* **2013**, *5* (1), 62−80.
(18) Hansen, T. W.; Wagner, J. B.; Hansen, P. L.; Dahl, S.; Topsøe, H.; Jacobsen, C. J. H. *Science* **2001**, *294*, 1508−1510.
(19) Neurock, M. *J. Catal.* **2003**, *216*, 73−88.
(20) Christensen, C. H.; Norskov, J. K. *J. Chem. Phys.* **2008**, *128*, 182503.
(21) Studt, F.; Abild-Pedersen, F.; Bligaard, T.; Sorensen, R. Z.; Christensen, C. H.; Nørskov, J. K. *Science* **2008**, *320*, 1320−1322.
(22) Nørskov, J. K.; Bligaard, T.; Hvolbaek, B.; Abild-Pedersen, F.; Chorkendorff, I.; Christensen, C. H. *Chem. Soc. Rev.* **2008**, *37*, 2163−2171.
(23) Nørskov, J. K.; Bligaard, T.; Rossmeisl, J.; Christensen, C. H. *Nat. Chem.* **2009**, *1*, 37−46.
(24) Nørskov, J. K.; Abild-Pedersen, F.; Studt, F.; Bligaard, T. *Proc. Natl. Acad. Sci. U. S. A.* **2011**, *108*, 937−943.
(25) Greeley, J.; Mavrikakis, M. *Nat. Mater.* **2004**, *3*, 810−815.
(26) Corma, A.; Boronat, M.; Gonzalez, S.; Illas, F. *Chem. Commun.* **2007**, 3371−3373.
(27) Chopra, I. S.; Chaudhuri, S.; Veyan, J. F.; Chabal, Y. J. *Nat. Mater.* **2011**, *10*, 884−889.
(28) Besenbacher, F.; Chorkendorff, I.; Clausen, B. S.; Hammer, B.; Molenbroek, A. M.; Nørskov, J. K.; Stensgaard, I. *Science* **1998**, *279*, 1913−1915.
(29) Chen, M. S.; Kumar, D.; Yi, C. W.; Goodman, D. W. *Science* **2005**, *310*, 291−293.
(30) Gao, F.; Wang, Y. L.; Li, Z. J.; Furlong, O.; Tysoe, W. T. *J. Phys. Chem. C* **2008**, *112*, 3362−3372.
(31) Tierney, H. L.; Baber, A. E.; Kitchin, J. R.; Sykes, E. C. H. *Phys. Rev. Lett.* **2009**, *103*, 246102.
(32) Tierney, H. L.; Baber, A. E.; Sykes, E. C. H. *J. Phys. Chem. C* **2009**, *113*, 7246−7250.
(33) Bellisario, D. O.; Han, J. W.; Tierney, H. L.; Baber, A. E.; Sholl, D. S.; Sykes, E. C. H. *J. Phys. Chem. C.* **2009**, *113*, 12863−12869.
(34) Kyriakou, G.; Boucher, M. B.; Jewell, A. D.; Lewis, E. A.; Lawton, T. J.; Baber, A. E.; Tierney, H. L.; Flytzani-Stephanopoulos, M.; Sykes, E. C. H. *Science* **2012**, *335*, 1209−1212.
(35) Lennard-Jones, J. E. *Trans. Faraday Soc.* **1932**, *28*, 333−359.
(36) Ramos, M.; Martinez, A. E.; Busnengo, H. F. *Phys. Chem. Chem. Phys.* **2012**, *14*, 303−310.
(37) Kresse, G.; Furthmüller, J. *J. Comput. Mater. Sci.* **1996**, *6*, 15−50.
(38) Kresse, G.; Furthmüller, J. *Phys. Rev. B* **1996**, *54*, 11169−11186.
(39) Blöchl, P. E. *Phys. Rev. B* **1994**, *50*, 17953−17979.
(40) Perdew, J. P.; Wang, Y. *Phys. Rev. B* **1992**, *45*, 13244−13249.
(41) Perdew, J. P.; Burke, K.; Ernzerhof, M. *Phys. Rev. Lett.* **1996**, *77*, 3865−3868.
(42) Haas, P.; Tran, F.; Blaha, P. *Phys. Rev. B* **2009**, *79*, 085104.
(43) Duncan, D. A.; Bradley, M. K.; Unterberger, W.; Kreikemeyer-Lorenzo, D.; Lerotholi, T. J.; Robinson, J.; Woodruff, D. P. *J. Phys. Chem. C* **2012**, *116*, 9985−9995.
(44) Henkelman, G.; Uberuaga, B. P.; Jónsson, H. *J. Chem. Phys.* **2000**, *113*, 9901−9904.
(45) Henkelman, G.; Jónsson, H. *J. Chem. Phys.* **1999**, *111*, 7010−7022.
(46) Tersoff, J.; Hamann, D. R. *Phys. Rev. B* **1985**, *31*, 805−813.
(47) Köhler, L.; Kresse, G. *Phys. Rev. B* **2004**, *70*, 165405.
(48) Kresse, G., Marsman, M., Furthmüller, J., Eds.; *VASP the Guide*; Computational Physics, Faculty of Physics, Universität Wien: Vienna, Austria, 2012.
(49) Zemlyanov, D.; Aszalos-Kiss, B.; Kleimenov, E.; Teschner, D.; Zafeiratos, S.; Hävecker, M.; Knop-Gericke, A.; Schlögl, R.; Gabasch, H.; Unterberger, W.; Hayek, K.; B., K. *Surf. Sci.* **2006**, *600*, 983−994.
(50) Groβ, A.; Dianat, A. *Phys. Rev. Lett.* **2007**, *98*, 206107.
(51) Groβ. *Phys. Rev. Lett.* **2009**, *103*, 246101.
(52) Aaen, A. B.; Laegsgaard, E.; Ruban, A. V.; Stensgaard, I. *Surf. Sci.* **1998**, *408*, 43−56.
(53) Hammer, B.; Nørskov, J. K. *Adv. Catal.* **2000**, *45*, 71−129.
(54) Kitchin, J. R.; Nørskov, J. K.; Barteau, M. A.; Chen, J. G. *Phys. Rev. Lett.* **2004**, *93*, 156801.